Learning a forest of Hierarchical Bayesian Networks to model dependencies between genetic markers

Raphaël Mourad, Christine Sinoquet, Philippe Leray

Learning a forest of Hierarchical Bayesian Networks to model dependencies between genetic markers

Raphaël Mourad†, Christine Sinoquet‡, Philippe Leray†

†LINA, UMR CNRS 6241, Ecole Polytechnique de l'Université de Nantes, rue Christian Pauc, BP 50609, 44306 Nantes Cedex 3, France,
‡LINA, UMR CNRS 6241, Université de Nantes, 2 rue de la Houssinière, BP 92208, 44322 Nantes Cedex, France

— KnOwledge and Decision (KOD) —

LABORATOIRE D'INFORMATIQUE DE NANTES ATLANTIQUE

RESEARCH REPORT

N° hal-00444087

January 2010

UNIVERSITÉ DE NANTES

ECOLE DES MINES DE NANTES

CENTRE NATIONAL DE LA RECHERCHE SCIENTIFIQUE

Raphaël Mourad†, Christine Sinoquet‡, Philippe Leray†

Learning a forest of Hierarchical Bayesian Networks to model dependencies between genetic markers

26 p.

Les rapports de recherche du Laboratoire d'Informatique de Nantes-Atlantique sont disponibles aux formats PostScript® et PDF® à l'URL :
http://www.sciences.univ-nantes.fr/lina/Vie/RR/rapports.html

Research reports from the Laboratoire d'Informatique de Nantes-Atlantique are available in PostScript® and PDF® formats at the URL:
http://www.sciences.univ-nantes.fr/lina/Vie/RR/rapports.html

Learning a forest of Hierarchical Bayesian Networks to model dependencies between genetic markers

Raphaël Mourad†, Christine Sinoquet‡, Philippe Leray†

raphael.mourad,christine.sinoquet,philippe.leray@univ-nantes.fr

Abstract

We propose a novel probabilistic graphical model dedicated to represent the statistical dependencies between genetic markers, in the Human genome. Our proposal relies on building a forest of hierarchical latent class models. It is able to account for both local and higher-order dependencies between markers. Our motivation is to reduce the dimension of the data to be further submitted to statistical association tests with respect to diseased/non diseased status. A generic algorithm, CFHLC, has been designed to tackle the learning of both forest structure and probability distributions. A first implementation of CFHLC has been shown to be tractable on benchmarks describing 10^5 variables for 2000 individuals.

1 Introduction

Genetic markers such as SNPs are the key to dissecting the genetic susceptibility of complex diseases: they are used for the purpose of identifying combinations of genetic determinants which should accumulate among affected subjects. Generally, in such combinations, each genetic variant only exerts a modest impact on the observed phenotype, the interaction between genetic variants and possibly environmental factors being determining in contrast. Decreasing genotyping costs now enable the generation of hundreds of thousands of genetic variants, or SNPs, spanning whole Human genome, accross cohorts of cases and controls. This scaling up to genome-wide association studies (GWAS) makes the analysis of high-dimensional data a hot topic. Yet, the search for associations between single SNPs and the variable describing case/control status requires carrying out a large number of statistical tests. Since SNP patterns, rather than single SNPs, are likely to be determining for complex diseases, a high rate of false positives as well as a perceptible statistical power decrease, not to speak of untractability, are severe issues to be overcome.

The simplest type of genetic polymorphism, Single Nucleotide Polymorphism (SNP), involves only one nucleotide change, which occurred generations ago within the DNA sequence. To fix ideas, we emphasize that one single individual can be uniquely defined by only 30 to 80 independent SNPs and unrelated individuals differ in about 0.1% of their 3.2 billion nucleotides. Compared with other kinds of DNA markers, SNPs are appealing because they are abundant, genetically stable and amenable to high-throughput automated analysis. Consistently, advances in high-throughput SNP genotyping technologies lead the way to various down-stream analyses, including GWASs.

Exploiting the existence of statistical dependencies between SNPs, also called linkage disequilibrium (LD), is the key to association studies achievement (Balding (2006)). Indeed, a causal variant may not be a SNP. For instance, insertions, deletions, inversions and copy-number polymorphisms may be causative of disease susceptibility. Nevertheless, a well-designed study will have a good chance of including one or more SNPs that are in strong LD with a common causal variant. In the latter case, indirect association with the phenotype, say affected/unaffected status, will be revealed (see Figure 1).

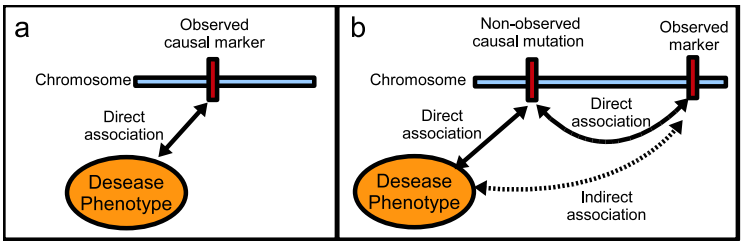

Figure 1: a) Direct association between a genetic marker and the phenotype. b) Indirect association between a genetic marker and the phenotype.

Interestingly, LD is also the key to reduce data dimensionality in GWASs. In eukaryotic genomes, LD is highly structured into the so-called "haplotype block structure" (Patit *et al.* (2001)): regions where correlation between markers is high alternate with shorter regions characterized by low correlation (see Figure 2). Relying on this feature, various approaches were proposed to achieve data dimensionality reduction: testing association with haplotypes (*i.e.* inferred data underlying genotypic data) (Schaid (2004)), partitioning the genome according to spatial correlation (Pattaro *et al.* (2008)), selecting SNPs informative about their context, or SNP tags (Han *et al.* (2008)) (for other references, see Liang *et al.*

(2008) for example). Unfortunately, these methods do not take into account all existing dependencies since they miss higher-order dependencies.

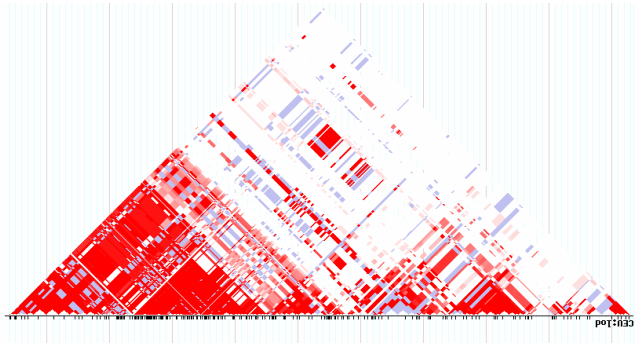

Figure 2: LD plot (matrix of pairwise dependencies between genetic markers or linkage disequilibrium). Human genome, chromosome 2, region [234 357kb - 234 457kb]. For a pair of SNPs, the colour shade is all the darker as the correlation between the two SNPs is high.

Probabilistic graphical models offer an adapted framework for a fine modelling of dependencies between SNPs. Various models have been used for this peculiar purpose, mainly Markov fields (Verzilli *et al.* (2006)) and Bayesian networks (BNs), with the use of hierarchical latent BNs (embedded BNs (Nefian (2006)); two-layer BNs with multiple latent (hidden) variables (Zhang and Ji (2009)). Although modelling SNP dependencies through hierarchical BNs is undoubtedly an attractive lead, there is still room for improvement. Notably, scalability remains a crucial issue.

In this paper, we propose to use a forest of Hierarchical Latent Class models (HLCMs) to reduce the dimension of the data to be further submitted to association tests. Basically, latent variables capture the information born by underlying markers. To their turn, latent variables are clustered into groups and, if relevant, such groups are subsequently subsumed by additional latent variables. Iterating this process yields a hierarchical structure. First, the great advantage to GWASs is that further association tests will be chiefly performed on latent variables. Thus, a reduced number of variables will be examined. Second, the hierarchical structure is meant to efficiently conduct refined association testing: zooming in through narrower and narrower regions in search for stronger association with the disease ends pointing out the potential markers of interest.

However, most algorithms dedicated to HLCM learning fail the scalability criterion when data describe thousands of variables and a few hundreds of individuals. The contribution of this paper is twofold: (i) the modelling of dependencies between clusters of SNPs, (ii) the design of a tractable algorithm, CFHLC, fitted to learn a forest of HLCMs from spacially-dependent variables. In the line of a hierarchy-based proposal of Hwang and collaborators (Hwang *et al.* 2006), our method yet implements data subsumption, meeting two additional requirements: (i) more flexible thus more faithful modelling of underlying reality, (ii) control of information decay due to subsumption. Section 2 motivates the design of HLCMs. Section 3 points out the few anterior works devoted to HLCM learning. Then, after an unformal description of the FHLC model, Section 4 focuses on the general outline of the method proposed for FHLCM learning. In Section 5, we give the sketch of algorithm CFHLC. Section 6 presents experimental results and discusses them.

2 Motivation for HLC modelling

From now on, we will restrain to discrete variables (either observed or latent).

A Latent Class Model (LCM) is defined as containing a unique latent variable connected to each of the observed variables. The latent variable influences all observed variables simultaneously and hence renders them dependent. In the LCM framework, an underlying assumption states that the observed variables are pairwise independent, conditional on the latent variable (Zhang (2004)). Since each state of the latent variable corresponds to a class of individuals, this assumption, also called local independence (LI), can be restated as pairwise independency, conditional on latent class membership. The intuition behind LI is that the latent variable is the only reason for the dependencies between observed variables. However, this assumption is often violated for observed data. To tackle this issue, HLCMs were proposed as a generalization of LCMs. HLCMs are tree-shaped BNs where leaf nodes are observed while internal nodes are not. In a Bayesian network, local dependency between variables may be modelled through the use of an additional latent variable (see Figure 3). At a larger scale, multiple latent variables organized in a hierarchical structure allow high modelling flexibility. Figure 4 illustrates the ability of HLCMs to depict a large variety of relations encompassing local to higher-order dependencies.

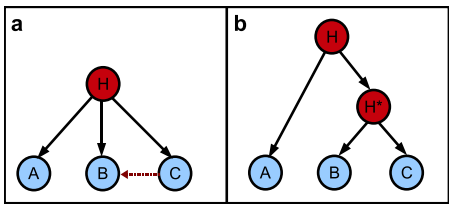

Figure 3: (a) Latent Bayesian network modelling a local dependency between B and C nodes. (b) Modelling of the local dependency between B and C nodes through a latent hierarchical model.

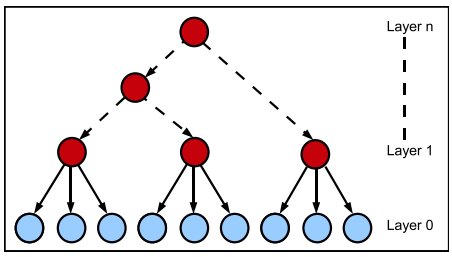

Figure 4: Hierarchical latent lodel. The light shade indicates the observed variables whereas the dark shade points out the latent variables.

3 Background for HLC model learning

Various methods have been conceived to tackle HLCM learning. These approaches differ by the following points: (i) structure learning; (ii) determination of the latent variables' cardinalities; (iii) learning of parameters, *i.e.* unconditional and conditional probabilities; (iv) scalability; (v) main usage.

As for general BNs, besides learning of parameters (θ), *i.e.* unconditional and conditional probabilities, one of the tasks in HLCM learning is structure ($\mathcal{S}$) inference. The HLCM learning methods fall into one of two categories. The first category, structural Expectation Maximization (SEM), successively optimizes $\theta \mid \mathcal{S}$ and $\mathcal{S} \mid \theta$. Amongst few proposals, hill-climbing guided by a scoring function was designed (Zhang (2003)): the HLCM space is visited through addition or removal of latent nodes alternating with addition or dismissing of states for existing nodes. Other authors adapted a SEM algorithm combined with simulated annealing to learn a two-layer BN with multiple latent variables (Zhang and Ji (2009)). Alternative approaches implement ascending hierarchical clustering (AHC). Relying on pairwise correlation strength, Wang and co-workers first build a binary tree; then they apply regularization and simplification transformations which may result in subsuming more than two nodes through a latent variable (Wang *et al.* (2008)). Hwang and co-workers' approach confines the HLCM search space to binary trees augmented with possible connections between siblings (nodes sharing the same parent into immediate upper layer) (Hwang *et al.* (2006)). Moreover, they constrain latent variables' arity to binarity. However, the latter approach is the only one we are aware of that succeeds in processing high-dimensional data: in an application dealing with a microarray dataset, more than 6000 genes have been processed for around 60 samples. To our knowledge, no running time was reported for this study.

Nevertheless, the twofold binarity restriction and the lack of control for information decay as the level increases are severe drawbacks to achieve realistic SNP dependency modelling and subsequent association study with sufficient power.

4 Constructing the FHLC model

4.1 The FHLC model

The HLCMs offer several advantages for GWASs. Beside data dimensionality reduction, they allow a simple test of direct dependency beween an observed variable and a target variable such as the phenotype, conditional on the latent variable, parent of the observed variable. Note that the phenotype variable is not included in the HLCM. In the context of GWASs, this test helps finding the markers which are directly associated with the phenotype, i.e. causal markers, should there be any. Second, the hierarchical structure allows zooming in through narrower and narrower regions in search for stronger association with the disease. This zooming process ends pointing out the potential markers of interest. Thirdly, the latent variables may be interpreted in a biological meaning. For instance, in the case of haplotypes, that is, phased genotypes, the latent variables are likely to represent the so-called haploblock structure of LD.

However, SNP dependencies would rather be more wisely modelled through a Forest of HLCMs (FHLCM), best accounting for possible higher-order dependencies on the genome. Indeed, in the case of a forest, higher-order dependencies are captured only when relevant, *i.e* when meeting a strength criterion. Also, not the least advantage over the HLC model lies in that variables are not constrained to be dependent upon one another, either directly or indirectly. Therefore, FHLCMs allow to model a larger set of configurations than HLCMs do. Typically, an HLCM is limited to manage LD structure modelling where clusters of close SNPs are dependent whereas no dependency exists between groups of distant SNPs or SNPs located on different chromosomes. But realistic modelling requires a more flexible framework. For instance, the six LD plots shown in Figure 5 give the intuition of the local dependency while also illustrating various cases of inter-dependency between clusters of SNPs.

An FHLCM consists of a Directed Acyclic Graph (DAG), also called the structure, whose non-connected components are trees, and of θ, the parameters (further defined). Figure 6 illustrates a possible

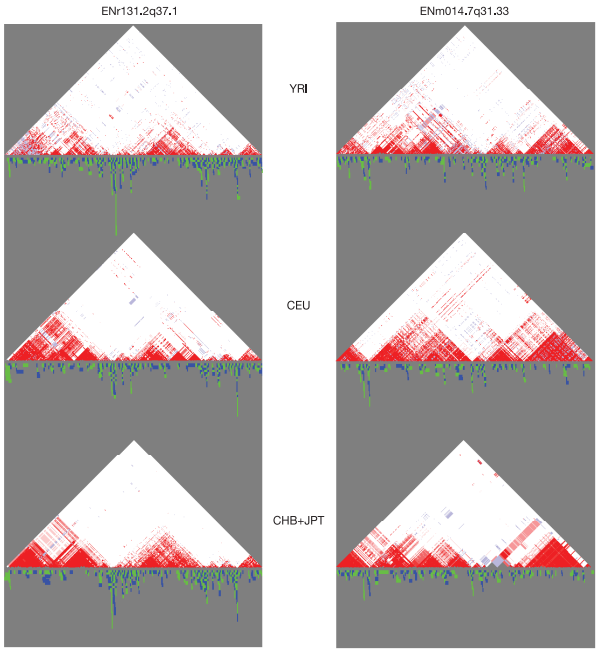

Figure 5: LD plot (matrix of LD measures for each pair of SNPs) in regions Encode ENr131.2q37.1 and ENm014.7q31.33 for the three populations YRI, CEU and CHB+JPT of the HapMap project (http://hapmap.ncbi.nlm.nih.gov/). The darker the shade, the stronger the LD.

structure for an FHLCM.

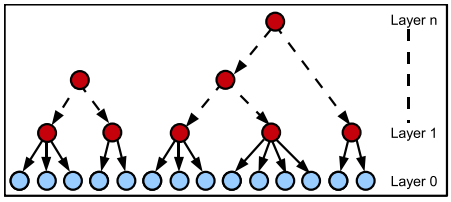

Figure 6: A forest of hierarchical latent models. This forest consists of two trees, of respective heights 2 and 3.

4.2 Principle

Our method takes as an input a matrix D_X defined on a finite discrete domain, say $\{0,\ 1,\ 2\}$ for SNPs, describing n individuals through p variables ($X = X_1, ..., X_p$). Algorithm CFHLC yields an FHLCM, that is a forest structure and θ, the parameters of a set of *a priori* distributions and local conditional distributions allowing the definition of the joint probability distribution. Two search spaces are explored: the space of directed forests and the probability space. In addition, the whole set of latent variables H of

the FHLCM is output, together with the associated imputed data matrix.

To handle high-dimensional data, our proposal combines two strategies. The first strategy splits up the genome-scale data into contiguous regions. In our case, splitting into (large) windows is not a mere implementational trick; it meets biological grounds: the overwhelming majority of dependencies between genetic markers (including higher-order dependencies) is observed for close SNPs. Then, an FHLCM is learnt for each window in turn. Within a window, subsumption is performed through an adapted AHC procedure: (i) at each agglomerative step, a partitioning method is used to identify clusters of variables; (ii) each such cluster is intended to be subsumed into an latent variable, through an LCM. For each LCM, parameter learning and missing data imputation (for the latent variable) are performed.

4.3 Node partitioning

Following Martin and VanLehn (1995), ideally, we would propose to associate a latent variable with any clique of variables in the undirected graph of dependency relations exhibiting pairwise dependencies of strengths being above a given threshold (see Figure 7). However, searching for such cliques is an NP-hard task. Moreover, in contrast with the previous authors' objective, FHLCMs do not allow clusters to have more than one parent each: non-overlapping clusters are required for our purpose. Thus, an approximate method solving a *partitioning* problem when provided pairwise dependency measures must be used.

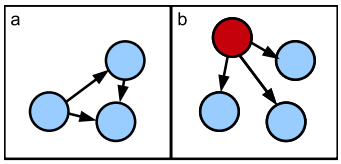

Figure 7: (a) Three pairwise dependent variables (clique). (b) Latent model: the three variables depend on a common latent variable. The dark shade indicates the latent variable designed to model the pairwise dependency between the three variables.

4.4 Parameter learning and imputation

A steep task is choosing - ideally optimizing - the cardinality of each LCM's latent variable. Instead of using an arbitrary constant value common to all latent variables, we propose that the cardinality be adapted for each latent variable through a function of the underlying cluster's size. The underlying rationale for choosing this function is the following: the more child nodes a latent variable has, the larger is the number of latent class value assignments for the child nodes. Therefore, the cardinality of this latent variable should depend on the number of child nodes. Nonetheless, to keep the model complexity within reasonable limits, a maximal cardinality is fixed.

Parameter learning is carried out step by step, each time generating additional latent variables and imputing their values for each individual. At i^{th} step, this task simply amounts to performing parameter learning for as many LC models as there are clusters of variables identified. We recall that the nodes in the topology of an LCM reduce to a root and leaves. Therefore, at i^{th} step, each LCM's structure is rooted in a newly created latent variable. When latent variables are only source nodes in a BN, parameter learning may be performed through a standard EM procedure. This procedure takes as an input the cardinalities of the latent variables and yields the probability distributions: *prior* distributions for those nodes with no

parents and distributions conditional to parents for the remaining nodes. After imputing the missing data corresponding to latent variables, new data are available to seed next step of the FHLCM construction: latent variables identified through step i will be considered as observed variables during step $i+1$.

It has to be noted that designing an imputation method to infer the values of the latent variable for each individual is in itself an investigation subject. Once the *prior* and conditional distributions have been estimated for a given LCM, probabilistic inference in BNs may be performed. A straightforward way would consist in imputing for each individual the latent variable value as follows: $h^* = argmax_h\{p(H = h/X_{j_1} = x_{j_1}, X_{j_2} = x_{j_2}, ..., X_{j_c} = x_{j_c})\}$. However, in the framework of probabilistic models, this deterministic approach is disputable. In contrast, a more convincing alternative will draw a value h for latent variable H, knowing the probabilities $p(H = h/X_{j_1} = x_{j_1}, X_{j_2} = x_{j_2}, ..., X_{j_c} = x_{j_c})$ for each individual.

4.5 Controlling information decay

In contrast with Hwang and co-workers' approach, which mainly aims at data compression, information decay control is required: any latent variable candidate H in step i which does not bear sufficient information about its child nodes must be unvalidated. As a consequence, such child nodes will be seen as isolated nodes in step $i+1$. The information criterion, $\mathcal{C}$, relies on average mutual information $\mathcal{I}$. It is scaled through entropy $\mathcal{H}$: $\mathcal{C} = \frac{1}{s_H} \sum_{i \in cluster(H)} \frac{\mathcal{I}(X_i,H)}{\min(\mathcal{H}(X_i), \mathcal{H}(H))}$, with s_H the size of $cluster(H)$.

5 Sketch of algorithm CFHLC

The user may tune various parameters: s, the window size, specifies the number of contiguous SNPs (*i.e.* variables) spanned per window; t is meant to constrain information dilution to a minimal threshold criterion $\mathcal{C}$, described in Subsection 4.5. Parameters a, b and $card_{max}$ participate in the calculus of the cardinality of each latent variable. Finally, parameter *PartitioningAlg* enables flexibility in the choice of the method devoted to cluster highly-correlated variables into non-overlapping groups.

Within each successive window, the AHC process is initiated from a first layer of univariate models. Each such univariate model is built for any observed variable in the set W_i (lines 4 to 6). The AHC process stops if all clusters identified each reduce to a single node (line 10) or if no cluster of size strictly greater than 1 could be validated (line 23). Each cluster of at least two nodes is subject to LCM learning followed by validation (line 13 to 22). In order to simplify the FHLCM learning, the cardinality of the latent variable is estimated as an affine function of the number of variables in the corresponding cluster (line 14). Algorithm *LCMLearning* is plugged into this generic framework (line 15). After validation through threshold t (lines 16 and 17), the LCM is used to enrich the FHLCM associated with current window (line 18): (i) a specific merging process links the additional node corresponding to the latent variable to its child nodes; (ii) the *prior* distributions of the child nodes are replaced with distributions conditional to the latent variable. In W_i, clusters of variables are replaced with the corresponding latent variables; data matrix $D[W_i]$ is updated accordingly (lines 19 and 20). In contrast, the nodes in unvalidated clusters are kept isolated for the next step. At last, the collection of forests, DAG, is successively augmented with each forest built within a window (line 24). In parallel, due to assumed independency between windows, the joint distribution of the final FHLCM is merely computed as the product of the distributions associated with windows (line 24).

Algorithm $CFHLC(X, D_X, s, t, PartitioningAlg, a, b, c_{max})$

INPUT:
$\mathbf{X}, \mathbf{D_X}$: a set of p variables $X = X_1, ..., X_p$ and the corresponding data observed for n individuals,
$\mathbf{s}$: a window size,
$\mathbf{t}$: a threshold used to limit information decay while building the FHLC,
$\mathbf{a}, \mathbf{b}, \mathbf{c_{max}}$: parameters used to calculate the cardinality of latent variables.

OUTPUT:
DAG, θ: the DAG structure and the parameters of the FHLC model constructed,
H, D_H: the whole set of latent variables identified through the construction ($H = \{H_1, ..., H_m\}$) and the corresponding data imputed for the n individuals.

1: $numWin \leftarrow p/s$;
2: $DAG \leftarrow \emptyset$; $\theta \leftarrow \emptyset$; $H \leftarrow \emptyset$; $D_H \leftarrow \emptyset$
3: **for** $i = 1$ **to** $numWin$
4: $W_i \leftarrow \{X_{(i-1)\times s+1}, ..., X_{i\times s}\}$; $D[W_i] \leftarrow D[(i-1)\times s + 1 : i \times s)]$
5: $\{\cup_{j\in W_i} DAG_{univ_j}, \cup_{j\in W_i} \theta_{univ_j}\} \leftarrow LearnUnivariateModels(W_i)$
6: $DAG_i \leftarrow \cup_{j\in W_i} DAG_{univ_j}$; $\theta_i \leftarrow \cup_{j\in W_i} \theta_{univ_j}$

7: $step \leftarrow 1$
8: **while true**
9: $\{C_1, ..., C_{nc}\} \leftarrow Partitioning(W_i, D[W_i], PartitioningAlg)$
10: **if** all clusters have size 1 **then break end if**

11: $C_{j_1}, ..., C_{j_{nc_2}} \leftarrow ClustersContainingAtLeast2Nodes(C_1, ..., C_{nc})$
12: $nc_{2_{valid}} \leftarrow 0$
13: **for** k = 1 **to** nc_2
14: $card_H \leftarrow min(RoundInteger(a \times NumberOfVariables(C_{j_k}) + b, c_{max})$
15: $\{DAG_{j_k}, \theta_{j_k}, H_{j_k}, DH_{j_k}\} \leftarrow LCMLearning(C_{j_k}, D[C_{j_k}], card_H)$
16: **if** $(\mathcal{C}(DAG_{j_k}, D[C_{j_k}] \cup DH_{j_k}) \geq t)$ /* validation of current cluster - see Section 4.5 */
17: $incr(nc_{2_{valid}})$
18: $DAG_i \leftarrow MergeDags(DAG_i, DAG_{j_k})$; $\theta_i \leftarrow MergeParams(\theta_i, \theta_{j_k})$
19: $H \leftarrow H \cup H_{j_k}$; $D_H \leftarrow D_H \cup DH_{j_k}$
20: $D[W_i] \leftarrow (D[W_i] \setminus D[C_{j_k}]) \cup DH_{j_k}$; $W_i \leftarrow (W_i \setminus C_{j_k}) \cup H_{j_k}$
21: **end if**
22: **end for**
23: **if** $(nc_{2_{valid}} = 0)$ **then break end if**

24: $DAG \leftarrow DAG \cup DAG_i$; $\theta \leftarrow \theta \times \theta_i$
25: $incr(step)$
26: **end while**

27: **end for**

Algorithm $LCMLearning(C_r, D[C_r], card_H)$

1: $H_r \leftarrow CreateNewLatentVariable()$
2: $DAG_r \leftarrow BuildNaiveStructure(H_r, C_r)$
3: $\theta_r \leftarrow standardEM(DAG_r, D[C_r], card_H)$
4: $DH_r \leftarrow Imputation(\theta_r, D[C_r])$

Table 1: Sketch of algorithm CFHLC.

6 Experimental results and discussion

Algorithm CFHLC has been implemented in C++, relying on the ProBT library dedicated to BNs (http://bayesian-programming.org). We have plugged into CFHLC a partitioning method, CAST, designed by Ben-Dor and co-authors (1999). CAST is a clique partitioning algorithm originally developped for gene expression clustering. As an input, it requires a similarity matrix and a similarity cutoff t. The algorithm contructs the clusters one at a time. The authors define the affinity $a(x)$ of an element x to be the sum

of similarity values between x and the elements present in the current cluster C_{open}. x is an element of high affinity if $a(x) \geq t|C_{open}|$. Otherwise, x is an element of low affinity. To summarize, the algorithm alternates between adding high affinity elements to C_{open} and removing low affinity elements from it. When the process stabilizes, C_{open} is closed. A new cluster can be started.

We have generated simulated genotypic data using software HAPSIMU (http://l.web .umkc.edu/ liujian/). The default values for HAPSIMU parameters have been kept. They are recapitulated in Table 2.

disease model parameters	disease prevalence	0.01
	genotype relative risk	1.5
	frequency of disease susceptible allele	min: 0.1, max: 0.3
population structure model parameters	proportion of YRI in cases	0.4
	proportion of YRI in controls	0.6
	number of generations	5
	frequency difference	min: 0.1, max: 0.3
simulation parameters	sample size (number of individuals)	**2000**
	proportion of cases in total sample	0.5
	simulating times	1
	genotype missing rate	0

Table 2: Parameter value adjustment for the generation of simulated genotypic data through software HAPSIMU.

CFHLC was run on a standard PC (3.8 GHz, RAM 3.3 Go). Three sample sizes were chosen to evaluate the scalability with respect to the number of observed variables: $1k$, $10k$ and $100k$ (In all cases, the number of individuals is set to 2000). For the first round of experimentations, a rough adjustment of the CFHLC parameters has been performed. Hereafter, the default setting for CFHLC parameters is the following: $a = 0.2,\ b = 2, c_{max} = 20,\ t = 0.5$. On the following figures, boxplots have been produced from 20 benchmarks (exceptionally 5 in the $100k$ case of Figure 8).

6.1 Temporal complexity

In the hardest case ($100k$), Figure 8 shows that only 15 hours are required with a window size s set to 100. The previous figure highlights very low variances, indicated through boxplots. For the same dataset processed in the cases "$s = 200$" and "$s = 600$", running times are 20.5 h and 62.5 h, respectively. For the same number of OVs ($100k$), Wang *et al.* report running times in the order of two months. Figure 9 more thoroughly describes the influence of window size increase on running time. In the current version of CFHLC algorithm, successive windows are contiguous. For a given window size, the temporal complexity of CFHLC is expected to be linear with respect to the number of variables. However, on the basis of an execution time of 20 mn for 1000 SNPs when s is set to 100, one would expect a running time of about 33 h for 10^5 SNPs. Following the same rationale, the expected running time for window size 200 should be around 42 h (in comparison to the observed execution time of 20.5 h). For window size 600, the expected running time to be compared to the observed running time of 62.5 h is 92 h. The corresponding values for the ratio of observed running time to expected running time are the following ones: 15 / 33 = 0.45 ($s = 100$); 20.5 / 42 = 0.49 ($s = 200$); 62.5 / 92 = 0.68 ($s = 600$). The existence of such ratios lead us to think that compression data may be drastic within many windows: the density of the dependency relations along the genome is heterogeneous.

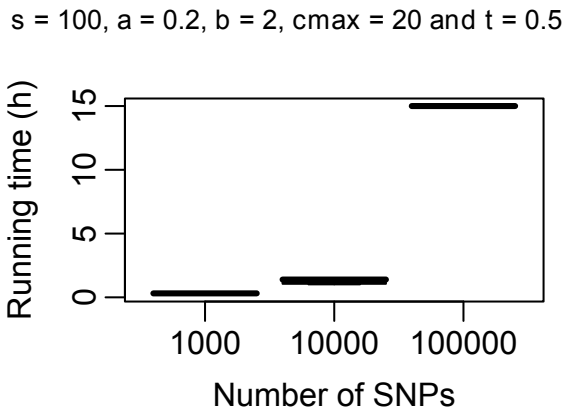

Figure 8: Running time versus number of variables. Low variances are highlighted through the boxplots drawn.

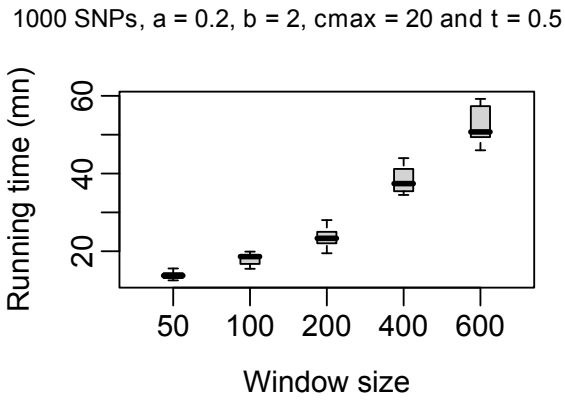

Figure 9: Impact of window size on running time.

6.2 Spacial complexity

We observe a dramatical decrease of the number of latent variables per layer (over the whole FHLCM) with the layer. Figure 10 exhibits this decrease in the case "$s = 100$". A percentage of 64% of the latent variables are present in the first layer. In particular, the decrease between first and second layers amounts to 60%. It has to be noted that although the number of latent variables is reduced, compared to Hwang and co-workers' algorithm, additional memory allocation is requested to account for the distributions of the non binary latent variables. However, the datasets of size $100k$ could be managed by our algorithm.

6.3 Impact of window size

Interestingly, Figure 11 highlights the decrease in the number of variables to be tested for association with the disease (from 1000 observed variables to less than 200 forest roots in the case "$s = 100$"). In this case, algorithm CFHLC allows a reduction in the number of variables of more than 80%.

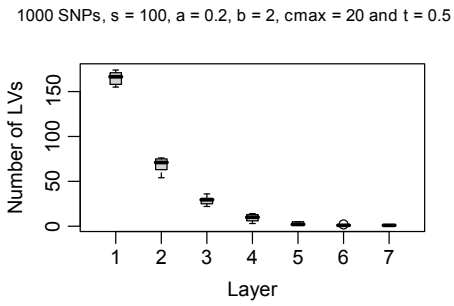

Figure 10: Number of latent variables per layer over the whole FHLC model.

Like the number of latent variables, the number of layers increases with the window size, as shown in Figures 12 and 13. This increase with window size is due to the fact that more higher-order interactions are taken into account. In average, around 270 latent variables and 5 to 6 layers are reported for the case "$s = 100$", whereas around 340 latent variables and 8 layers are identified for the case "$s = 600$".

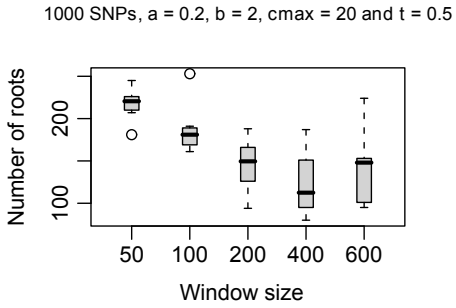

Figure 11: Impact of window size on the number of roots.

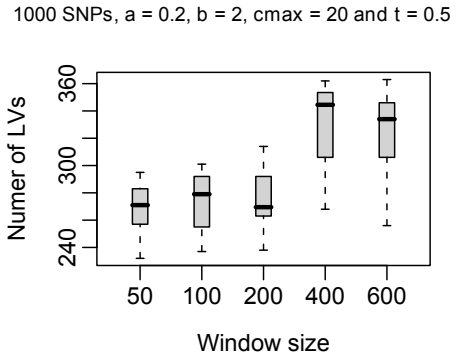

Figure 12: Impact of window size on the number of latent variables.

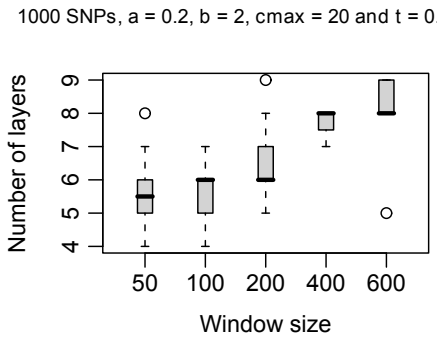

Figure 13: Impact of window size on the number of layers.

Figure 14 provides a more thorough insight of the distributions of latent variables between layers. Figure 14(a) shows the impact of window size on the number of latent variables in a given layer while Figure 14(b) plots the ratios of the number of latent variables per layer to the total number of latent variables. Again, we observe a constant result: for all layers except the first one, the numbers (and ratios) are all the higher as the window size is larger. The exception relative to first layer is explained as follows: for a constant parameter setting of the partitioning algorithm, when the number of observed variables increases, that is when the window size increases, the number of clusters identified is smaller (with larger sizes).

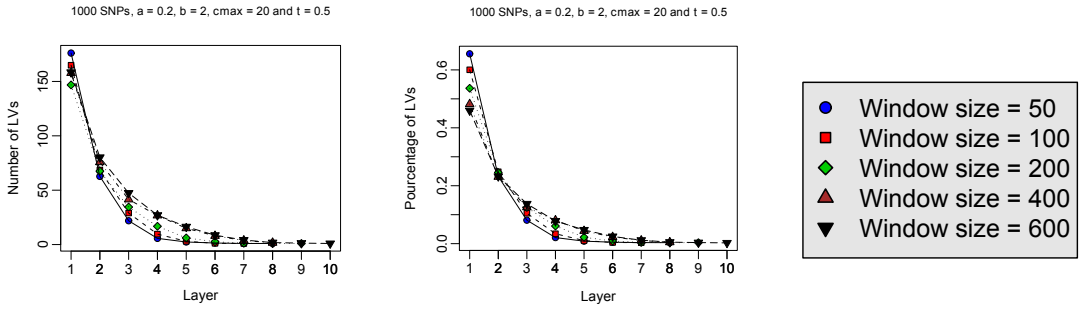

(a) (b)

Figure 14: (a) Average number of latent variables per layer over the whole FHLC model; impact of window size. (b) Average ratio of the number of latent variables per layer to the total number of latent variables; impact of window size.

6.4 Quality of the model

Figure 15, 16 and 17 display how information fades while the layer number increases. Regarding window size 600, the four first layers show average values around 0.62, 0.60, 0.59 and 0.58 for the scaled mutual information-based score $\mathcal{C}$ (see Figure 15). In the highest layers, average scaled mutual information is at least equal to 0.52 and 0.56 for the cases "$s = 100$" and "$s = 600$" respectively. Therefore, not only is a major point reached regarding tractability, information dilution is also controlled in an efficient way. The increasing variance is explained by the decreasing number of latent variables involved in the average calculation (see Figure 10). In the highest layers, this sampling effect is all the more acute, entailing such

variations as that observed for layer 8 and window size 50. In the latter case, a unique latent variable has been considered to compute the mean; it happened that the mutual information-based score calculated was outstandingly high in comparison with other values.

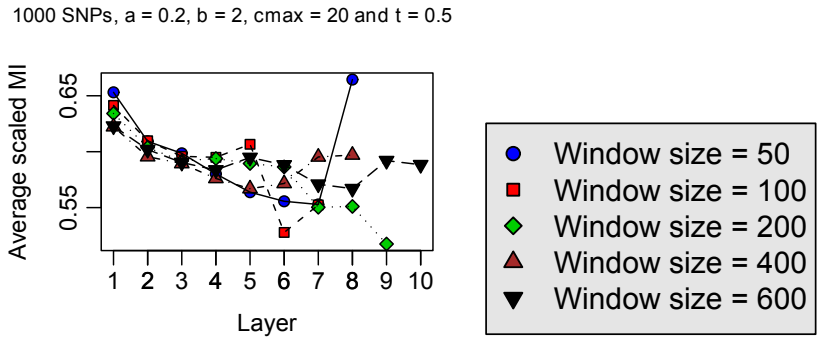

Figure 15: Average scaled mutual information per layer over the whole FHLC model; impact of window size.

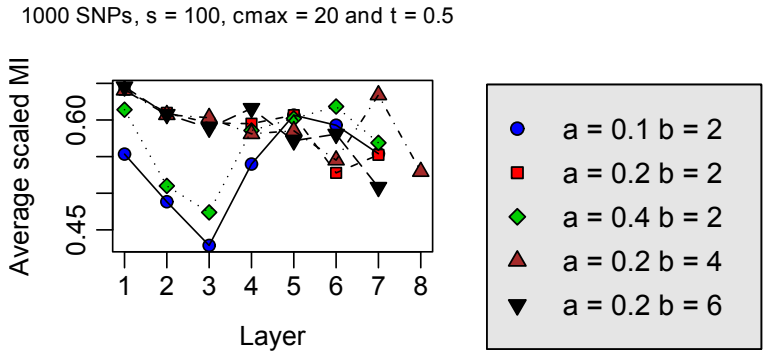

Figure 16: Average scaled mutual information per layer over the whole FHLC model; impact of parameters a and b.

As expected, average scaled mutual information raises with parameters a and b because latent variables with larger cardinalities allow to capture more information about their child nodes, in the FHLCM (see Figure 16). Besides, in the absence of information decay control, that is when threshold t is set to 0, the average criterion $\mathcal{C}$ shows a particular trend: it first decreases throughout the first three layers then it increases while traversing fourth layer to highest layer (Figure 17). Up to the third layer, a latent variable captures less and less information about its child nodes as the layer number rises: a loss of information is therefore observed. In contrast, latent variables in higher layers subsume but a few number of child nodes since clusters are smaller. Hence, these latent variables can easily provide sufficient information about their child variables. In addition, we observe that criterion $\mathcal{C}$ never goes down lower than 0.36. Expecting the constant conservation of more than a third of shared information between child and parent nodes was not foreseeable. Nonetheless, this observation advocates the importance of controlling information decay.

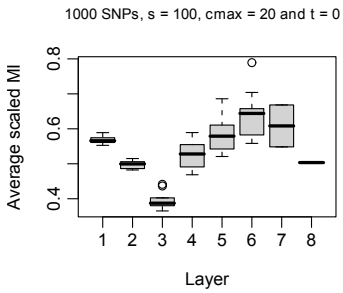

Figure 17: Average scaled mutual information per layer over the whole FHLC model; absence of information decay control ($t = 0$).

A refined optimization of the adjustment of parameters a and b justifies in itself a thorough study and therefore lies beyond the scope of the present work. First, given a dataset, some investigations in wider ranges of values for a and b parameters must be performed: theoretically, the optimized values would ensure the lowest information dilution over the whole corresponding FHLCM constructed. In practice, for efficiency, a discretized search will have to be adapted.

Conversely, for a more refined analysis of the information decay through layers, we plan to run complementary tests on various datasets, under the *same parameter setting* of a, b and t. Besides, Hwang and co-workers have published a figure similar to Figure 15 (Hwang *et al* (2006), Figure 3(a)), where the four first layers respectively exhibit $\mathcal{C}$ values around 0.65, 0.55, 0.52 and 0.51. Acknowledging the bias due to the differences in the datasets used by these authors and in our experimentations (see Figure 15), we observe similar orders of magnitude. In contrast to standard AHC, CFHLC allows flexible thus *early* node clustering; therefore, if ever existing in the binary model and the FHLCM, the latent variable subsuming a given cluster of nodes should be harboured at a lower level in our approach than in standard AHC; it follows that information dilution is expected to be delayed when using CFHLC. To thoroughly check this point, in the future, we will compare both decreases of $\mathcal{C}$ in a systematic study, running Hwang and co-workers' algorithm and ours on the same datasets.

6.5 Examples of FHLC networks

Finally, Figure 18, 19 and 20 display examples of DAGs of FHLCMs obtained for window sizes set to 100, 200 and 600, respectively. The software Tulip (http://tulip.labri.fr/TulipDrupal/) was chosen to visualize the DAGs, meeting both high representation quality and compactness requirements. For all window sizes, several trees of various sizes are observed, and generally, we observe that the SNPs which share the same parent are close on DNA. Thereby, the large trees represent the high correlation regions, whereas trees with only one or two SNPs correspond to low correlation regions of LD, also called recombination hotspots. Algorithm CFHLC discovers 3, 4 and 6 layers of dependencies for window sizes 100, 200 and 600 respectively. As expected, the larger the window, the more refined the LD modelling is.

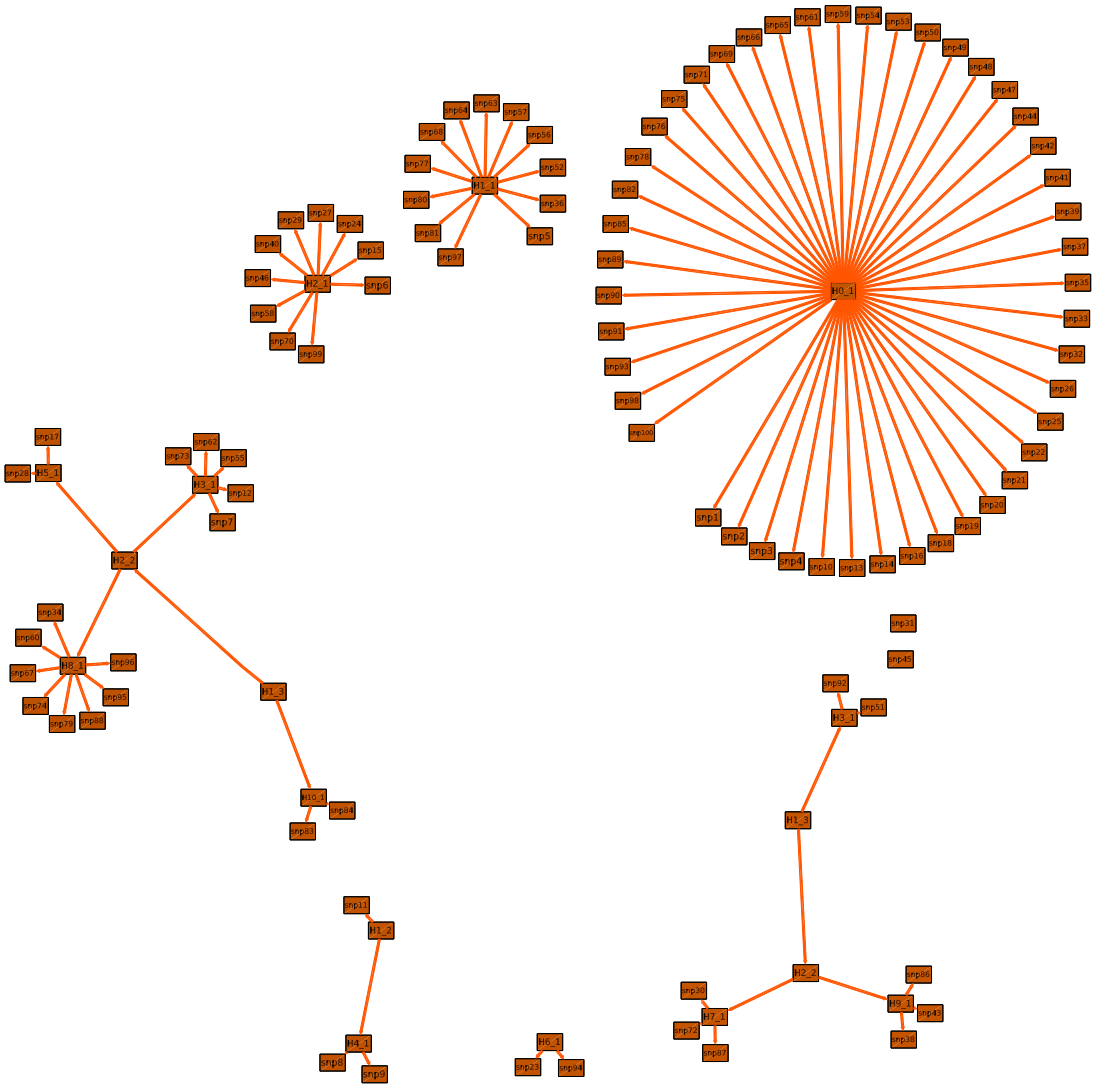

Figure 18: Directed acyclic graph of the FHLC model learned for window size 100. Observed variables are named ”snp_i” whereas latent variables are denoted ”Hi_l” where i enumerates the different latent variables belonging to a same layer and l specifies the layer number.

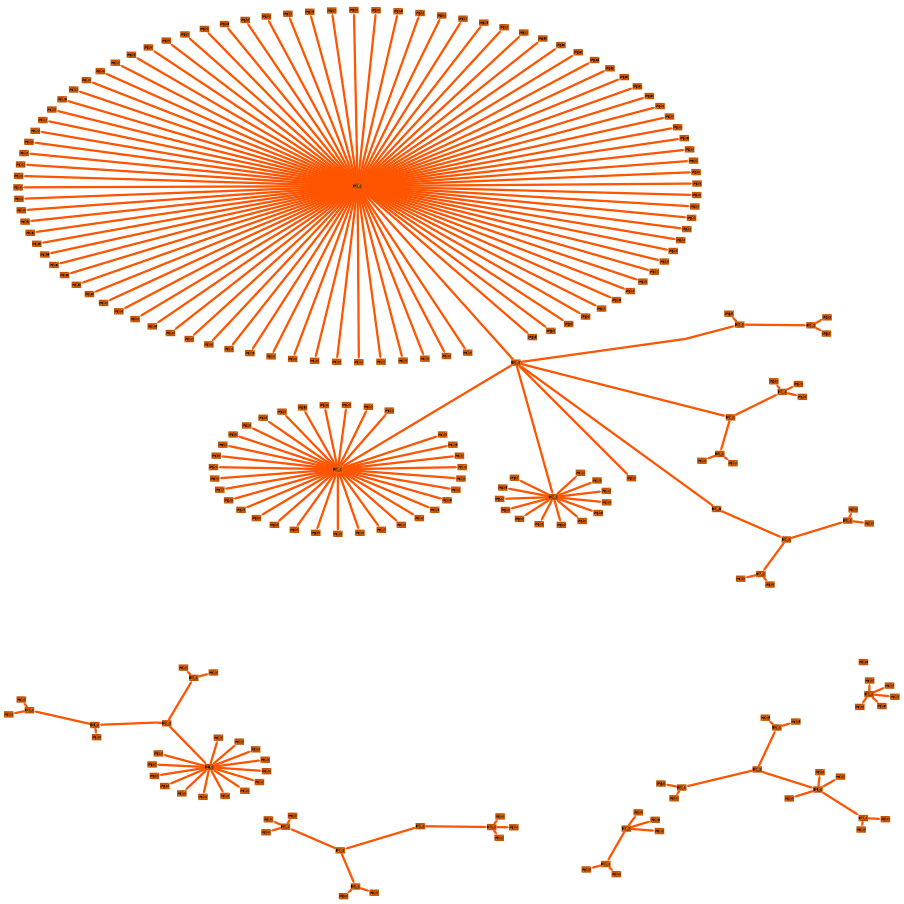

Figure 19: Directed acyclic graph of the FHLC model learned for window size 200. See Table 18 for node nomenclature.

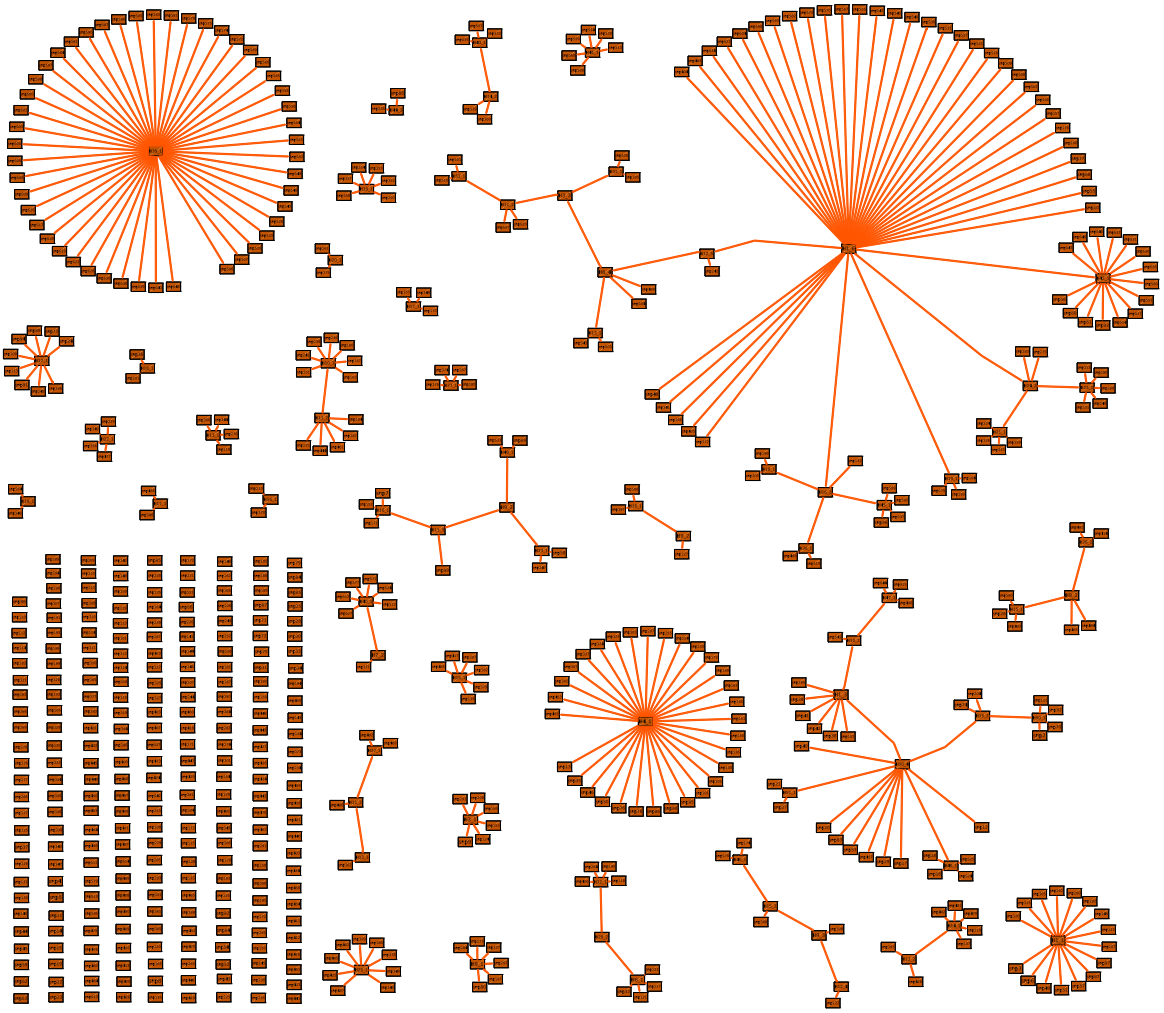

Figure 20: Directed acyclic graph of the FHLC model learned for window size 600. See Table 18 for node nomenclature.

7 Conclusion and perspectives

Our contribution in this paper is twofold: (i) a variant of the HLC model, the FHLC model, has been described; (ii) CFHLC, a generic algorithm dedicated to learn such models, has been shown to be efficient when run on genome-scaled benchmarks.

To our knowledge, our hierarchical model is the first one shown to achieve fast model learning for genome-scaled data sets while maintaining satisfying information scores. Whereas Hwang and collaborators' purpose is data compression, we are faced with a more demanding challenge: allow a sufficiently powerful down-stream association analysis. Relaxing the twofold binarity restriction of Hwang and collaborators' model (binary trees, binary latent variables), the FHLC model is an appealing framework for GWASs: in particular, flexibility in the cluster size reduces the number of latent variables.

A bottleneck currently lies in the clustering method chosen, which forbids window sizes encompassing more than 600 observed variables. In addition to investigating alternative clustering methods, a lead to cope with this bottleneck may be to adapt some specific processing at the limits of contiguous windows or use overlapping windows.

Regarding node partitioning and imputation for latent variables, one of our current tasks is examining which plug-in methods are most relevant, especially for the purpose of GWASs. Also, in complement to this work-on progress paper, the next step will consist in a thorough analysis of the impact of the criterion designed to control information dilution. Finally, we will evaluate CFHLC as a promising algorithm enhancing genome wide genetic analyses, including study and visualization of linkage disequilibrium, mapping of disease susceptibility genetic patterns and study of population structure.

References

BALDING, D.J. (2006). A tutorial on statistical methods for population association studies. *Nat. Rev. Genet., 7(10), 781-791, doi: 10.1038/nrg1916-c1*.

BEN-DOR, A., SHAMIR, R. and YAKHINI, Z. (1999): Clustering gene expression patterns. *Journal of Computational Biology 6(3-4), 281-97*.

HAN, B., KANG, H.M., SEO, M.S., ZAITLEN, N. and ESKIN, E. (2008): Efficient association study design via power-optimized tag SNP selection. *Ann Hum Genet. 72(6), 834-47*.

HWANG, K.B., KIM, B.-H. and ZHANG, B.-T. (2006): Learning hierarchical Bayesian networks for large-scale data analysis. *ICONIP (1), 670-679*.

LIANG, Y., KELEMEN, A. (2008): Statistical advances and challenges for analyzing correlated high dimensional SNP data in genomic study for complex diseases. *Statistics Surveys 2, 43-60*.

MARTIN, J. and VANLEHN, K. (1995). Discrete factor analysis: learning hidden variables in Bayesian networks. *Technical report, Department of Computer Science, University of Pittsburgh*.

NEFIAN, A.V. (2006): Learning SNP dependencies using embedded Bayesian networks, *Computational Systems Bioinformatics Conference CSB'2006*, Stanford, USA, poster.

PATIL, N., BERNO, A.J., HINDS, D.A., BARRETT, W.A., DOSHI, J.M., HACKER, C.R., KAUTZER, C.R., LEE, D.H., MARJORIBANKS, C., MCDONOUGH, D.P., NGUYEN, B.T.N., NORRIS, M.C., SHEEHAN, J.B., SHEN, N., STERN, D., STOKOWSKI, R.P., THOMAS, D.J., TRULSON, M.O., VYAS, K.R., FRAZER, K.A., FODOR, S.P.A., COX, D.R. (2001) Blocks of limited haplotype diversity revealed by high-resolution scanning of human chromosome 21. *Science 294, 1719-1723*.

PATTARO, C., RUCZINSKI, I., FALLIN, D.M., PARMIGIANI, G. (2008): Haplotype block partitioning as a tool for dimensionality reduction in SNP association studies. *BMC Genomics 9, 405, doi:10.1186/1471-2164-9-405*.

SCHAID, D.J. (2004): Evaluating associations of haplotypes with traits. *Genetic Epidemiology 27(4), 348-364*.

VERZILLI, C.J., STALLARD, N. and WHITTAKER, J.C. (2006): Bayesian graphical models for genomewide association studies. *American journal of human genetics, 79(1), 100-112*.

WANG, Y., ZHANG, N.L. and CHEN, T. (2008): Latent tree models and approximate inference in Bayesian networks. *Journal of Artificial Intelligence Research, 32(1), 879-900*.

ZHANG, N.L. (2003). Structural EM for hierarchical latent class model. *Technical report, HKUST-CS03-06.*

ZHANG, N.L. (2004). Hierarchical latent class models for cluster analysis. *The Journal of Machine Learning Research, 5(6):697-723*.

ZHANG, Y. and JI, L. (2009): Clustering of SNPs by a Structural EM Algorithm. *International Joint Conference on Bioinformatics, Systems Biology and Intelligent Computing, 147-150*.

Learning a forest of Hierarchical Bayesian Networks to model dependencies between genetic markers

Raphaël Mourad†, Christine Sinoquet‡, Philippe Leray†

Abstract

We propose a novel probabilistic graphical model dedicated to represent the statistical dependencies between genetic markers, in the Human genome. Our proposal relies on building a forest of hierarchical latent class models. It is able to account for both local and higher-order dependencies between markers. Our motivation is to reduce the dimension of the data to be further submitted to statistical association tests with respect to diseased/non diseased status. A generic algorithm, CFHLC, has been designed to tackle the learning of both forest structure and probability distributions. A first implementation of CFHLC has been shown to be tractable on benchmarks describing 10^5 variables for 2000 individuals.

LINA, Université de Nantes
2, rue de la Houssinière
B.P. 92208 — F-44322 NANTES CEDEX 3